# A Study of $e^+e^- \rightarrow H^0A^0$ Production at 1 TeV and the Constrain on Dark Matter Density

Marco Battaglia<sup>1,2</sup>, Benjamin Hooberman<sup>1</sup>, Nicole Kelley<sup>1</sup>

1- University of California - Dept of Physics, Berkeley, CA - USA

2- Lawrence Berkeley National Laboratory, Berkeley, CA - USA

### 1 Introduction

The connections between Cosmology and Particle Physics through Dark Matter (DM) have received special attention in the last few years for sharpening the physics case of collider physics at the TeV frontier. There are many extensions of the Standard Model (SM), which include a new, stable, weakly-interacting massive particle, possibly responsible for the observed relic DM in the Universe. The LHC will provide first important data to address the question whether one of these scenarios is indeed realised in nature. The ILC measurements of the properties of a DM candidate and of those other particles participating to its interactions in the early Universe may allow us to predict its relic density with an accuracy comparable to that currently achieved by CMB observations at satellites. With these data in hand, the comparison of the results would have striking consequences for our understanding of dark matter.

## 2 Neutralino Dark Matter Density in MSSM and the ILC

Supersymmetry emerges as the best motivated theory of new physics beyond the SM. It solves a number of problems, intrinsic to the SM and, most important to our discussion, the conservation of R-parity introduces a new stable, weakly interacting particle. The WMAP CMB data, and other astrophysical data, already set rather stringent bounds on Supersymmetry parameters, if the neutralino is responsible for saturating the amount of DM observed.

The potential of ILC data at 0.5 TeV and 1.0 TeV for determining the DM relic density,  $\Omega_{\chi}$ , in Supersymmetry has been investigated in detail in [1]. This study selected a set of benchmark points, the so-called LCC points, representative of various scenarios and determined the  $\Omega_{\chi}$  probability density function by a scan of the full MSSM parameter space and retaining those points compatible with the measurements available at the LHC and ILC within their accuracy.

# 3 $e^+e^- \rightarrow H^0 A^0$ at LCC-4 with Full Simulation

We consider here a specific Supersymmetric scenarios, in which the DM candidate is the lightest neutralino,  $\chi_1^0$  and its relic density is controlled by the rate of neutralino annihilation through the CP-even heavy Higgs pole  $\chi\chi \to A$ . The LCC-4 benchmark point [1] is defined in the cMSSM, corresponding to the parameters  $m_0=380.00 \text{ GeV}$ ,  $m_{1/2}=420 \text{ GeV}$ ,  $\tan \beta=53$ ,  $A=0, Sgn(\mu)=+1$  and  $M_{top}=178 \text{ GeV}$ . We use Isasugra 7.69 [2] to compute the particle spectrum and we get  $M_{A^0}=419.4 \text{ GeV}$ ,  $M_{\chi_1^0}=169.1 \text{ GeV}$  and  $M_{\tau_1}=195.5 \text{ GeV}$ . The  $e^+e^- \to$ 

 $H^0A^0 \rightarrow b\bar{b}b\bar{b}$  process at  $\sqrt{s} = 1$  TeV ILC has already been studied for LCC4 [3]. That study, based on the parametric detector simulation program Simdet 4.0, showed that the  $A^0$  boson mass can be determined to  $\pm 0.8$  GeV by imposing the natural width  $\Gamma_A$  or to  $\pm 2.0$  GeV by a simultaneous fit to mass and width. These results, when combined with other measurements to be peformed at 0.5 TeV, allow us to predict the neutralino contribution to the dark matter density in the Universe,  $\Omega_{\chi}$  to a relative accuracy of 18 % in generic MSSM scenarios.

Here, we repeat the same study on Geant-4-based simulation [4] of the detector response and reconstruct the physics objects using processors developed in the Marlin framework [5]. This study adopts the LDC detector concept, which employs a large continuous gaseous tracker Time Projection Chamber surrounded by a highly granular calorimeter and complemented by a high resolution Vertex Tracker, for which we have chosen the option based on CMOS monolithic pixel sensors. The LDC detector is discussed in details elsewhere [6], the design is optimised for achieving excellent parton energy measurements, through the particle flow algorithm, and precise extrapolation of particle tracks to their production point. Both these features are important to the analysis, which aims to suppress backgrounds by exploiting its signature 4-b jet final state and requires good determination of energy and direction of hadronic jets to maximise the resolution on di-jet invariant masses. The jet energy resolution has been studied using a simulated sample of single b jets in the energy range from 10 GeV to 210 GeV over a polar angle,  $\theta$ , range  $0.4 < \theta < \pi/2$ , we get  $\delta E/E = (0.34 \pm 0.02)/\sqrt{E} \oplus$  $(0.015 \pm 0.005)$ , which is consistent with the particle flow performance specifications. Jet flavour tagging is based on three observables: the probability for all the particle tracks to originate at the event primary vertex, the fraction of the jet energy carried by secondary particles and the  $p_t$ -corrected mass of the secondary particles. These are combined to form a discriminant variable which peaks at one for b jets and peaks at zero for non-b jets.

At the chosen working point, an efficiency for b jets of 85 % is obtained with sufficient rejection of lighter quarks to effectively suppress the remaining non-*b* background. Signal events have been generated with Pythia 6.205+Isajet 7.69, including bremsstrahlung effects. These events have been passed through the full LDC simulation using the Mokka 06-03 program [7] based on Geant-4. The lcio [8] collections produced by Mokka have been used as input for the Marlin reconstruction. At  $\sqrt{s}$ = 1 TeV, the effective  $e^+e^- \rightarrow$  $H^0 A^0$  production cross section, accounting for beamstrahlung, is 1.4 fb and the decay  $BR(A^0 \rightarrow b\bar{b})$ is 0.87. The main backgrounds are

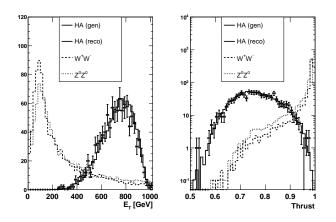


Figure 1: Tranverse energy and thrust distributions for HA,  $Z^0Z^0$  and  $W^+W^-$ . Generator level distributions are plotted as histograms, results of Mokka + Marlin simulation and reconstruction are given for the signal process as points with error bars.

 $Z^0 Z^0$ ,  $W^+ W^-$  production and the inclusive  $b\bar{b}b\bar{b}$  production. Their cross sections are 0.2 pb,

3.2 fb and 5.1 fb respectively. We assume to operate the ILC at 1 TeV for a total integrated luminosity of 2 ab<sup>-1</sup>. Backgrounds can be significantly suppressed using event shape and kinematic variables. We require events to fulfill the following criteria: total recorded energy in the event  $E_{TOT} > 850$  GeV, total transverse energy  $E_T > 350$  GeV, charged energy in the event  $E_{CHA} > 350$  GeV, number or reconstructed particles  $N_{TOT} > 50$ , number of charged particles  $N_{CHA} > 25$ , event thrust <.95 and  $Y_{34} < 0.0025$ , where  $Y_{34}$  is the 3 to 4 jet crossover value of the jet clustering variable. The distributions of some of these variables is shown in Figure 1) for backgrounds and signal, for which a comparison of the generator-level and reconstructed values is also given.

After event selection, the di-jet pairing which minimises the di-jet mass difference has been chosen. The di-jet mass resolution has been improved by applying a 4-C fit. We

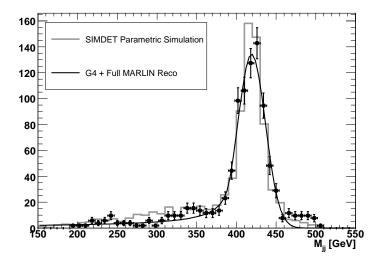


Figure 2: Dijet invariant mass distribution for  $e^+e^- \rightarrow H^0A^0$  events selected by the analysis cut. Mass constraint fit and jet flavour tagging has been applied. The distribution for fully simulated and reconstructed events (points with error bars) is compared to that obtained with parametric simulation (histogram).

have ported the PUFITC algorithm, developed for the DELPHI experiment at LEP, into a dedicated Marlin processor. The algorithm adjusts the momenta of the jets given by  $\vec{p}_F = e^a \vec{p}_M + b \vec{p}_B + c \vec{p}_C$  where  $\vec{p}_F$  is the fitted momentum,  $\vec{p}_M$  is the measured momentum,  $\vec{p}_B$ and  $\vec{p}_C$  are unit vectors transverse to  $\vec{p}_M$  and to each other, and a, b and c are the free parameters in the fit. The adjusted momenta satisfy a set of constraints while minimizing the fit  $\chi^2$ , which is given by  $\Sigma_i (a_i - a_0)^2 / \sigma_a^2 + b_i^2 / \sigma_b^2 + c_i^2 / \sigma_c^2$ , where  $a_0$  is the expected energy loss parameter,  $\sigma_a$  is the energy spread parameter and  $\sigma_b, \sigma_c$  are the transverse momentum spread parameters. In this analysis we use the following constraints:  $p_x = p_y = 0$  and  $E \pm |p_z| = \sqrt{s}$ , where the last condition accounts for beamstrahlung along the beam axis, z. We report here preliminary results from the analysis of a sample of 1050 fully simulated signal events. After applying final selection and mass constrained fit, the sample of eventss in the region 150 GeV  $M_{jj} < 550$  GeV gives a selection efficiency of 23 % for signal  $b\bar{b}\bar{b}$ 

LCWS/ILC 2007

decays. The resulting mass distribution is shown in Figure 2. We describe the signal as a CRYSTAL BALL (CB) function [9] and extract the  $A^0$  mass,  $M_A$ , and width,  $\Gamma_A$  have been by a multi-parameter fit leaving the CB parameters free. We determine the  $A^0$  mass as (419.1±0.9) GeV. This result is remarkably close to that obtained in the earlier analysis, based on parametric detector simulation. The production and analysis of fully simulated and reconstructed background samples is currently under way.

### 4 Further Constraints on $\Omega_{\chi}$

The constraints on LCC4 derived from mass measurements at the LHC and ILC, provide a prediction of the DM density in the Universe to a relative accuracy of 18 % with a generic MSSM model.

This accuracy is still far from that achieved by CMB study with satellites. The main contribution to the remaining uncertainty is the weak constrain which the data provide to MSSM solutions where  $\Omega_{\chi}$  is significantly lower than its reference for LCC4. A detailed study shows that these solutions are all characterised by large values of the stau trilinear coupling,  $A_{tau}$ . In the MSSM the  $\tilde{\tau}$  coupling to the  $H^0$  and  $A^0$  bosons scales as  $A_{tau} \frac{\cos \alpha}{\cos beta} + \mu \frac{\sin \alpha}{\cos \beta}$  and  $A_{tau} \tan \beta + \mu$ , respectively. In the funnel region the main annihilation mechanism is  $\tilde{\chi}^0 \tilde{\chi}^0 \rightarrow A^0 \rightarrow$  $b\bar{b}$  and  $M_A < M_{\tilde{\tau}_1} + M_{\tilde{\tau}_2}$ . The only  $A^0$  decay into  $\tilde{\tau}$ s, allowed by CP symmetry,  $A^0 \to \tilde{\tau}_1 \tilde{\tau}_2$  is kinematically forbidden. At large values of

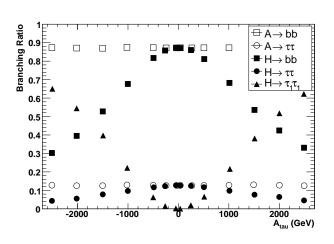


Figure 3:  $H^0$  and  $A^0$  decay branching fractions as a function of the stau trilinear coupling  $A_{tau}$  predicted by HDECAY. All the other MSSM parameters have been kept fixed to those corresponding to the LCC4 point.

 $|A_{tau}|$ , the stau decay process through the  $H^0 \rightarrow \tilde{\tau}_1 \tilde{\tau}_1$  gets a sizeable branching fraction. This channel contributes to the neutralino annihilation rate through  $\tilde{\chi}^0 \tilde{\chi}^0 \rightarrow H^0 \rightarrow \tilde{\tau}_1 \tilde{\tau}_1$ , bringing down the corresponding relic density, as observed in the MSSM scans. At the same time, a determnation of the branching fraction of the decay  $H^0 \rightarrow \tilde{\tau}_1 \tilde{\tau}_1$ , allows to constrain  $|A_{tau}|$ . Figure 3 shows the decay branching fractions of the  $A^0$  and  $H^0$  bosons computed using the HDECAY 2.0 program [10] as a function of  $A_{tau}$ . Now, a large  $H^0 \rightarrow \tilde{\tau}_1 \tilde{\tau}_1 \rightarrow \tau \tilde{\chi}^0 \tau \tilde{\chi}^0$  yield can be detected by a standard  $b\bar{b}\tau\tau$  analysis. A preliminary study shows that the  $A^0$ ,  $H^0 \rightarrow \tau\tau$  branching fraction can be determined to  $\pm 15$  % and  $A^0$ ,  $H^0 \rightarrow b\bar{b}$  to  $\pm 7$  %, from which a limit  $|A_{tau}| < 250$  GeV can be derived. This constrain removes the tail at low values of  $\Omega_{\chi}$  and results in a prediction of the neutralino relic density with a relative accuracy of 8 %. A detailed study on full simulation to support these preliminary results is currently under way.

LCWS/ILC2007

### Acknowledgments

We are grateful to Abder Djouadi for pointing out the sensitivity of the H decay branching fractions to  $A_{tau}$  and to Michael Peskin for discussion. This work was supported by the Director, Office of Science, of the U.S. Department of Energy under Contract No.DE-AC02-05CH11231 and used resources of the National Energy Research Scientific Computing Center, supported under Contract No.DE-AC03-76SF00098.

### References

- E. A. Baltz, M. Battaglia, M. E. Peskin and T. Wizansky, Phys. Rev. D 74 (2006) 103521 [arXiv:hep-ph/0602187].
- [2] F. E. Paige, S. D. Protopopescu, H. Baer and X. Tata, arXiv:hep-ph/0312045.
- [3] M. Battaglia, arXiv:hep-ph/0410123.
- [4] S. Agostinelli et al., Nucl. Instrum. Meth. A 506 (2003), 250.
- [5] F. Gaede, Nucl. Instrum. Meth. A 559 (2006) 177.
- [6] Detector Outline Document for the Large Detector Concept, August 2006.
- [7] G. Musat, Prepared for International Conference on Linear Colliders (LCWS 04), Paris, France, 19-24 Apr 2004
- [8] F. Gaede, T. Behnke, N. Graf and T. Johnson, In the Proceedings of 2003 Conference for Computing in High-Energy and Nuclear Physics (CHEP 03), La Jolla, California, 24-28 Mar 2003, pp TUKT001 [arXiv:physics/0306114].
- [9] T. Skwarnicki, PhD thesis, DESY-F31-86-02 (1986).
- [10] A. Djouadi, J. Kalinowski and M. Spira, Comput. Phys. Commun. 108 (1998) 56 [arXiv:hep-ph/9704448].